Polyolefin blends: 2. Effect of EPR composition on structure, morphology and mechanical properties of iPP/EPR alloys

R. Greco, C. Mancarella, E. Martuscelli and G. Ragosta
Istituto di Ricerche su Tecnologia dei Polimeri e Reologia del CNR, Arco Felice, 80072 Naples, Italy

and Yin Jinghua
Changchun Institute of Applied Chemistry, Academia Sinica, China
(Received 13 October 1986; revised 4 March 1987; accepted 21 April 1987)

The morphology, thermal behaviour, tensile and impact properties of sheet specimens of isotactic polypropylene (iPP) blended with ethylene–propylene copolymers (EPR) containing different amounts of polypropylene or polyethylene blocks and various extents of crystallinity were investigated by means of optical and scanning electron microscopy, differential scanning calorimetry, wide-angle X-ray diffractometry, impact and tensile mechanical tests. The experimental results showed that copolymers containing polypropylene or polyethylene blocks could act as nucleating agents for iPP spherulites. It was found that the mode and state of dispersion of the EPR copolymers, as well as the thermal and mechanical behaviour of the blends, depended upon the composition of the copolymer used in the blends for given crystallization conditions. The observed behaviour is very similar to that reported for high-density polyethylene/ethylene–propylene copolymer blends in the first paper of this series. This allows us to discuss the results in terms of the generalized behaviour of such polyolefin blends.

(Keywords: polypropylene; ethylene–propylene copolymers; blends morphology; mechanical properties)

INTRODUCTION

In recent years a great deal of work has been carried out on binary blends containing as components isotactic polypropylene (iPP) and elastomers with different chemical structures[1–10], as these mixtures are of great interest from both an industrial and a scientific point of view. Under certain circumstances, the rubber modification of iPP with ethylene–propylene copolymer (EPR) can lead to a material with improved impact strength and environmental stress-cracking resistance[11].

In previous papers[1–6] we studied the crystallization behaviour, morphology and impact behaviour as well as the mechanical tensile response of binary blends containing iPP and a sample of a random ethylene–propylene copolymer with C_2/C_3 ratio of 1.6 (in moles). This copolymer showed only a small amount of crystallinity, accounted for by the fact that very short ethylene sequences were present along the chains.

The present paper, the second of this series, investigates the morphology, structure, thermal behaviour and mechanical properties of blends of iPP with ethylene (C_2)–propylene (C_3) copolymers having a variable C_2/C_3 ratio, thus containing different types (polypropylene or polyethylene) and extent of crystallinity. The aim of the paper is to study the influence of copolymer structure and the type of crystallinity on the crystallization, morphology, impact fracture behaviour and drawing process of isotactic polypropylene (iPP)/ethylene–propylene copolymer (EPR) blends.

The results are compared with those of high-density polyethylene (HDPE)/EPR blends analysed in the first paper[12] of the series.

EXPERIMENTAL

Material

Ethylene–propylene copolymers were synthesized by using the Ziegler–Natta catalyst, $TiCl_3$,$Al(C_2H_5)_2Cl$ (Al/Ti = 4/1). The concentration of the catalyst was 6 mmol l^{-1} (n-heptane solvent). The polymerization temperature was 50°C and polymerization time was 1 h. Only copolymers containing PP (or PE) blocks or long propylene (or ethylene) sequences along the molecular chain were synthesized. The characterization of copolymers is given in *Table 1*: from left to right, the code (letters are an abbreviation of ethylene–propylene (EP) and digits represent the percentage of propylene in moles), the percentage of propylene in weight, the feed ratio of monomers to the polymerization reactor, the intrinsic viscosity $[\eta]$, the crystallinity X_c, the melting temperature T_m (measured by d.s.c.) and the glass transition temperature T_g (measured by torsion pendulum) are reported.

Isotactic polypropylene (PPM 260) was produced by Exxon Chem. Co. with $\bar{M}_w = 440\,000$, $\bar{M}_n = 100\,000$ and $\bar{M}_w/\bar{M}_n = 4.4$.

Blend preparation

Blends of isotactic polypropylene and ethylene–propylene copolymer were prepared by melt mixing in a

0032-3861/87/111929-08$03.00

Table 1 Compositions and characterization of EPR copolymers

Code	C_3 content (wt%)	Feed ratio of monomers (C_2/C_3)	$[\eta]$ (dl g^{-1}) in decahydronaphthalene at 135°C	X_c (%)	T_m (°C)	T_g (°C)
EP-88	92	4/96	1.66	42[a]	143[a]	0 to 6
EP-81	86	14/86	1.83	15[a]	125[a]	−10
EP-74	81	22/78	1.67	4[a]	119[a]	−20
EP-66	74	32/68	2.08	3[a]	118[a]	−33
EP-55	65	44/56	1.65	2[b]	123[b]	−36
EP-16	22	75/25	3.73	27[b]	125[b]	−50

[a] iPP crystallinity
[b] PE crystallinity

Brabender-like apparatus (Haake Rheocord instrument). The blending temperature was 200°C, blending time was 15 min and rotor rate was 32 rpm.

Specimen preparation

Specimens for mechanical tensile tests. The blended material was hot-pressed in a hydraulic press (Wabash) at 200°C and 240 kg cm^{-2}. The sheets obtained were about 1 mm thick. Dumbbell specimens were cut from the sheets and used for the mechanical property investigation. The tensile mechanical tests were all performed on blends having the same 80/20 (iPP/EP) weight ratio.

Specimens for impact tests. First the blended materials with different compositions and iPP/EPR weight ratios were hot-pressed in the same hydraulic press at 200°C and at a pressure of 240 kg cm^{-2}. The moulded sheets obtained were 3.0 mm thick. Then Charpy-type specimens 6.0 mm wide and 60 mm long were cut by a saw from the sheets.

Finally all the specimens were notched at the middle of their length as follows: a blunt notch was made by a slotter machine and then a very sharp notch 0.2 mm deep was produced by a razor blade fixed on a micrometer apparatus. The final value of the notch depth was measured after fracture by using an optical microscope.

For the impact studies the following blends were prepared: iPP/EP-88 and iPP/EP-55 with 100/0, 90/10, 85/15 and 80/20 (w/w) compositions.

Specimens for d.s.c. experiments. Specimens were obtained by quenching the molten samples down to room temperature in a water bath. Samples with a fibre morphology were cut from the middle of specimens elongated to a draw ratio of 6.50.

Specimens for morphology observations. The specimens used for optical microscopy were cut cryogenically with an LKB ultramicrotome. Those to be utilized for electron microscopy were cut by using a Reichert-Sung microtome. Specimens for SEM observation were etched using n-heptane vapour to remove the copolymers which contained more amorphous content.

Some specimens were etched with CrO_3/H_2SO_4 saturated solution at 80°C for 40–80 min to destroy the amorphous phase of the blended systems. The etching solution was prepared as follows. First the concentrated sulphuric acid (97% in weight) was diluted with water (H_2SO_4/water = 1:4). Then it was heated to 80°C and the CrO_3 added to form the saturated solution.

Techniques

Mechanical tensile tests. For the stretching tests on blends, an Instron machine (at room temperature with a crosshead speed of 10 mm min^{-1}) was used. The draw ratio for iPP and iPP/EPR blends was 6.50. Young's modulus E, yield strength σ_y and constant stress at cold-drawing σ_c were obtained from the stress–strain curves. The fibres formed by necking of the initial specimens were cut between the two necks and stretched by the Instron machine under the same operating conditions as above. Their Young's modulus E, tensile strength σ_b and elongation at break ε_b were also calculated from their stress–strain curves.

Impact fracture measurements. Charpy impact tests were carried out at a speed of 1 m s^{-1} by using a Ceast fracture pendulum. Samples with a notch depth-to-width ratio of 0.3 and a span test of 48 mm were fractured at different temperatures ranging from −100 to 20°C. The temperature was changed by means of a home-made liquid–nitrogen apparatus. Curves of impact strength as a function of test temperature were obtained for all the iPP/EP-55 and iPP/EP-88 blends.

D.s.c. measurements. Crystallinity X_c, melting temperature T_m, crystallization temperature T_c and width at half height of the melting and crystallization peaks were determined by using a Mettler TA 300 system apparatus. The rate of increasing and decreasing temperature was 20 K min^{-1}.

For the determination of the crystallization temperature T_c the specimens were heated to 230°C and kept at this temperature for 10 min and then cooled down to room temperature. The average weight of specimens was about 7 mg. For the calculation of crystallinity a value of $\Delta H° = 209$ J g^{-1} for iPP was used.

Morphology observations. Optical micrographs were taken by using a Wild M420 microscope. The surfaces of specimens observed by SEM were coated with Au–Pd and observed by a Philips 501-B scanning electron microscope.

WAXD measurements. Wide-angle X-ray diffraction (WAXD) measurements were performed by means of a Philips PW 1060/71 diffractometer (Ni-filtered CuKα radiation). The high voltage was 50 kV and tube current was 30 mA.

RESULTS AND DISCUSSION

Morphology

Optical micrographs of thin sections cut perpendicular to the plane of the moulded sheets of iPP, iPP/EP-88 and iPP/EP-16 blends are shown in *Figure 1*. These reveal that the average spherulite dimensions of the iPP phase

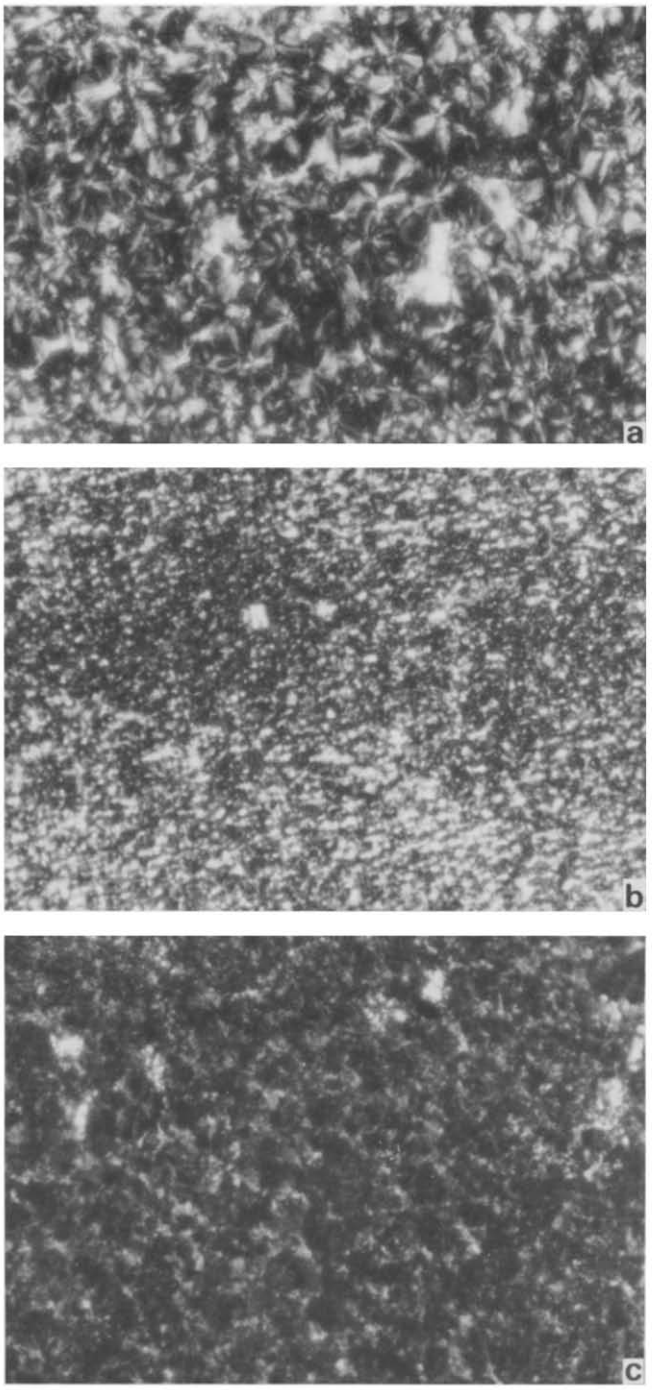

Figure 1 Optical micrographs (150 ×) of iPP and iPP/EPR copolymer blends: (a) iPP; (b) iPP/EP-88; (c) iPP/EP-16

are lower for the blends. This observation infers that EPR acts as a nucleating agent since we can exclude any possibility of heterogeneous nucleation from the eventual impurities contained in the copolymers. In fact elsewhere[1,3] the nucleating effect, for samples of iPP/EPR blends crystallized at a low undercooling, was effective only at C_3 levels lower than 66%. All the copolymers were obtained using the same synthesis procedure, and therefore we can exclude the possibility that foreign nucleants could be present to influence iPP nucleation. This observation is in agreement with our previous findings[1-3].

It is to be noted furthermore that such a reduction in spherulite size is dependent on C_3 content. In fact, the higher the percentage of C_3 the stronger is the nucleating effect of the matrix (see *Figures 2* and *3*).

SEM micrographs of thin sections (etched with n-heptane) of iPP, iPP/EP-16, iPP/EP-66, iPP/EP-74, iPP/EP-81 and iPP/EP-88 are shown respectively in *Figures 2–7*. For pure iPP no material could be etched out by boiling n-heptane after 20 min. After about 3 min for iPP/EP-16 blends a large amount of material was extracted by the dissolving power of boiling n-heptane. The sizes of the holes and craters are in the range 1–10 μm. The surfaces of the holes are very smooth.

This observation indicates that EP-16 segregates into droplet-like domains having poor adhesion to the iPP matrix. These domains are easily extracted by using boiling n-heptane due to the high C_2 content of EP-16, which renders the copolymer only very slightly compatible with the amorphous C_3 regions of iPP. From EP-66 to EP-88 (*Figures 4–7*) the C_3 content in the copolymers increases progressively and the number and size of holes in blends after etching with n-heptane decrease systematically. For iPP/EP-88 blends hardly anything could be extracted even after 30 min. These observations can be accounted for by assuming that with increase of the C_3 content in copolymers, even though the crystallinity of copolymers increases gradually, the compatibility in the

Figure 2 SEM micrographs of etched surfaces of iPP (n-heptane, 20 min) magnification 3600 ×

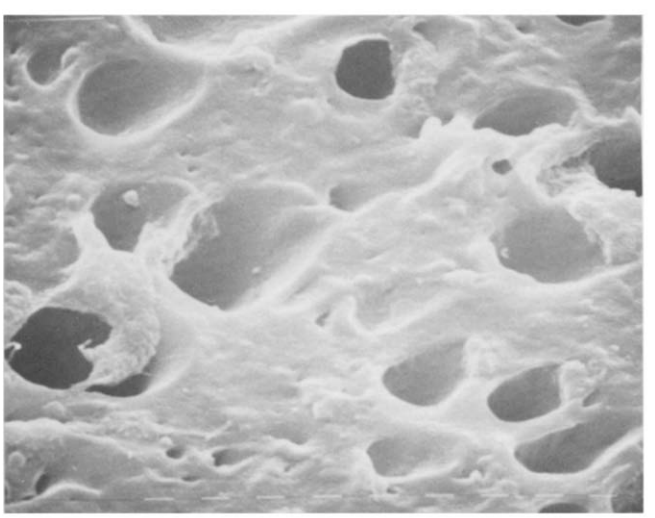

Figure 3 SEM micrographs of etched surfaces of iPP/EP-16 (n-heptane, 3 min) magnification 3600 ×

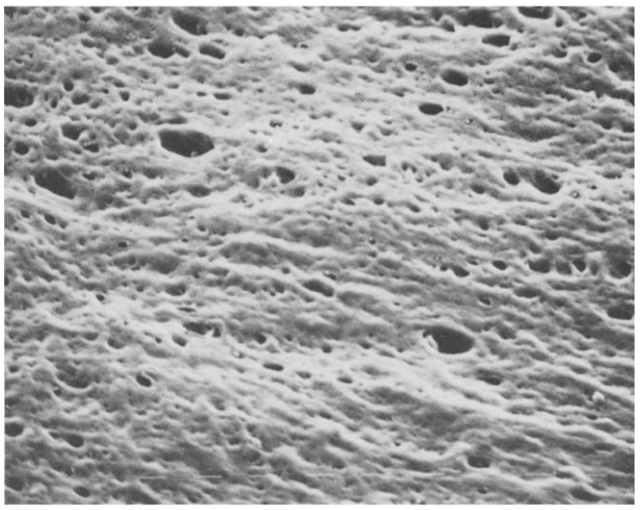

Figure 4 SEM micrographs of etched surfaces of iPP/EP-66 (n-heptane, 2 min) magnification 3600 ×

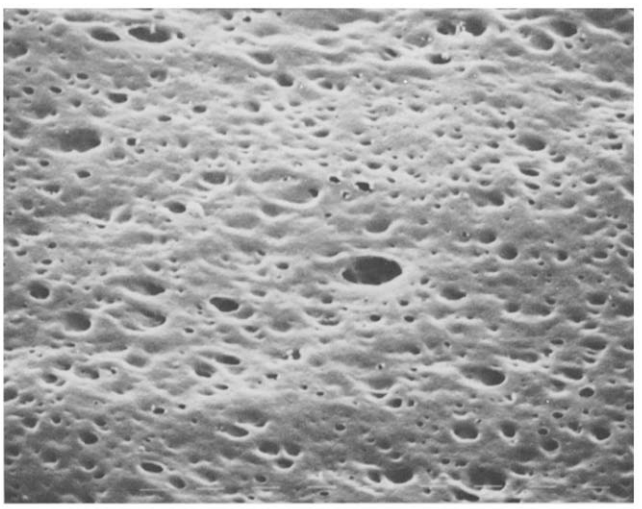

Figure 5 SEM micrographs of etched surfaces of iPP/EP-74 (n-heptane, 4 min) magnification 3600 ×

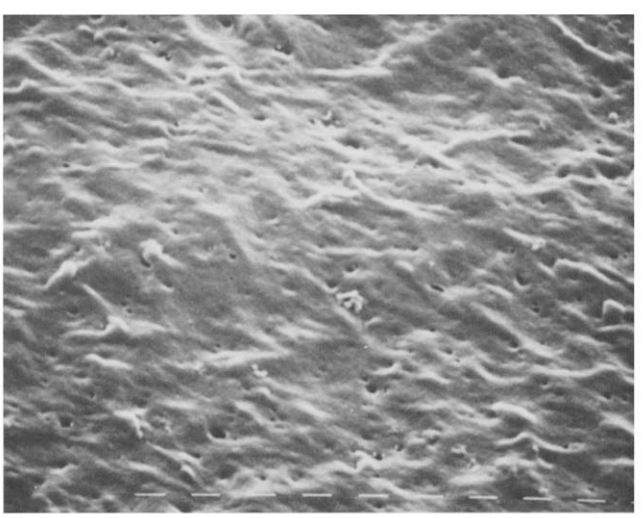

Figure 6 SEM micrographs of etched surfaces of iPP/EP-81 (n-heptane, 5 min) magnification 3600 ×

amorphous regions enhances progressively, making it more and more difficult to extract copolymer from the matrix.

The effect can be verified by using a different etch with strong oxidants (CrO_3/H_2SO_4). The analysis of electron micrographs of iPP, iPP/EP-88 and iPP/EP-81 blends (*Figures 8*, *9* and *10* respectively) shows that the size of pure iPP spherulites is larger and more compact

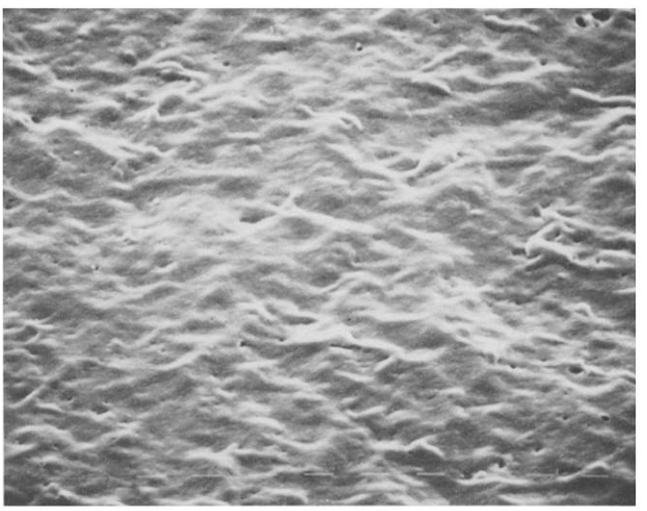

Figure 7 SEM micrographs of etched surfaces of iPP/EP-88 (n-heptane, 30 min) magnification 3600 ×

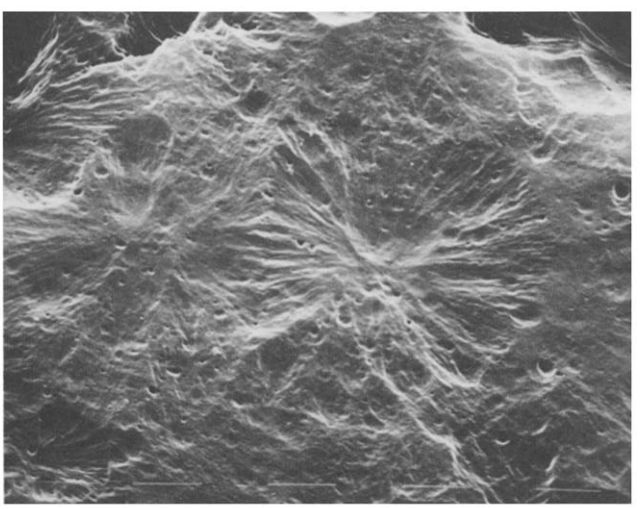

Figure 8 SEM micrographs of etched surfaces of iPP (CrO_3/H_2SO_4, 80 min, 80°C) magnification 900 ×

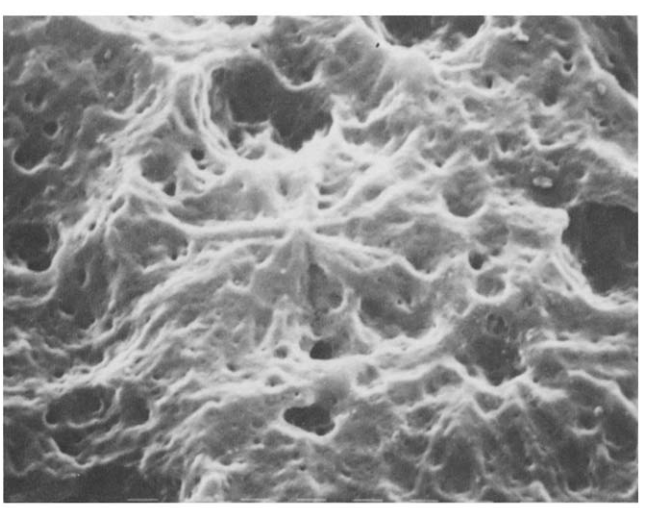

Figure 9 SEM micrographs of etched surfaces of iPP/EP-88 (CrO_3/H_2SO_4, 40 min, 80°C) magnification 3600 ×

compared to the spherulites in blends, which are more open and coarse. It is likely that amorphous material belonging to the copolymers is incorporated more and more into intraspherulite regions with increasing C_3 content of copolymers.

Thermal properties

The parameters calculated from the differential scanning thermograms are shown in *Table 2*: from left to right, the type of blend, the overall crystallinity X_c, the calculated crystallinity X_c^p (obtained by means of the following additivity equation, which assumes no interactions between the iPP and the copolymers: $X_c^p = W_{iPP}X_{c,iPP} + W_{EP}X_{c,EP}$), the melting and crystallization temperatures T_m and T_c, and the width at half height of the melting and crystallization peaks are shown.

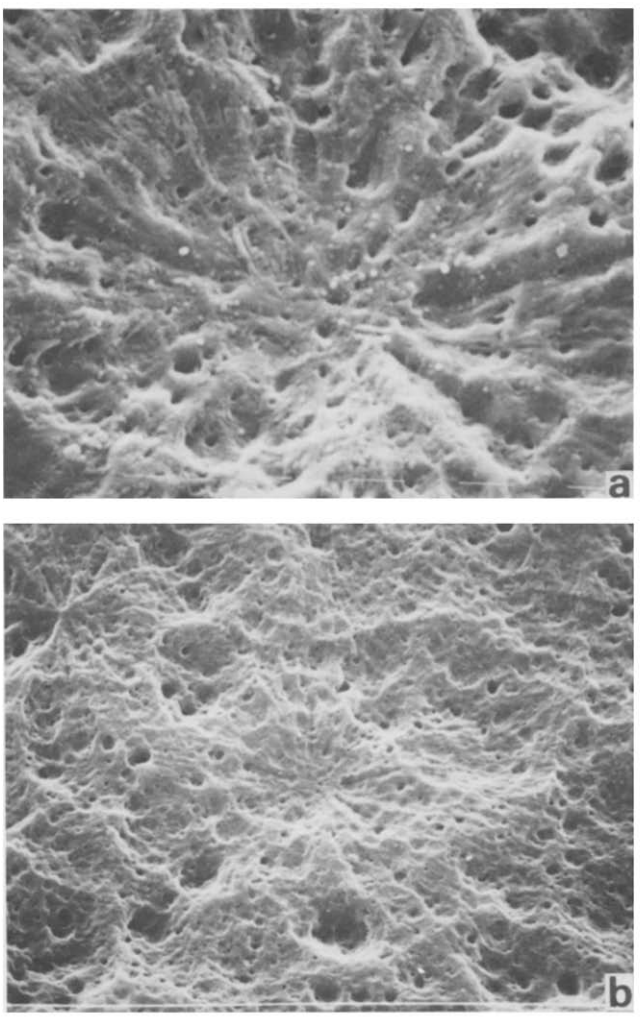

Figure 10 SEM micrographs of etched surfaces of iPP/EP-81 (CrO_3/H_2SO_4, 40 min, 80°C), (a) magnification 900×, (b) magnification 1900×

The overall crystallinity X_c determined by d.s.c. decreases for all the blends with respect to pure iPP. This is accounted for by the fact that 20% of iPP is substituted by less crystalline copolymers. As expected the calculated crystallinity (X_c^p) also decreases with increase of the C_2 content in the copolymer (EP-88, 81, 74, 66). The melting temperature of the crystallized phase in blends is 6–10 K higher than for plain iPP and the width at half height of the T_m peak is narrower for the blends than for pure iPP. In the case of the iPP/EP-16 blend a melting peak at a lower temperature, belonging to the PE crystallizing phase, is observed.

We can assume that the thermal behaviour of iPP/EPR blends can be attributed to the fact that during melt mixing in the Brabender-like apparatus the copolymers were able to dissolve a certain amount of iPP molecules having an average higher concentration of steric defects and/or a lower molecular weight. In other words, this means that copolymers may selectively extract from the iPP matrix more defective molecules, leaving a matrix of iPP molecules which, on average, have a higher degree of stereoregularity and a higher molecular mass. Therefore during pressure moulding and successive rapid crystallization, this kind of segregation is still retained. Therefore crystals of major perfection (higher T_m, lower width at half height of T_m peaks) are grown from the melt blends. As the iPP matrix in the blends loses a certain amount of crystallizable defective molecules and/or has lower molecular weights, the d.s.c. overall crystallinity is lower than the calculated crystallinity X_c^p. Furthermore these iPP defective molecules and the copolymers themselves seem to have lost almost all their crystallinity, since no melting peaks at lower temperatures (118–143°C) are detected and the iPP peak is displaced to higher temperatures and is narrower for the blends than for pure iPP. This effect on T_m and on the width at half height was observed for HDPE/EPR blends as well[12].

For the last blend (in *Table 2*), iPP/EP-16, double peaks (melting peaks) appeared in the differential scanning thermogram. The larger one is the T_m peak of the iPP matrix at a very high temperature (174°C), indicating in this case an even stronger extraction effect of the copolymer on iPP than in the other blends. The smaller one belongs to the ethylene blocks or long sequences present in the EP-16 copolymer. The crystallization thermogram of such blends shows only one crystallization peak. This is due to the fact that the two

Table 2 Crystallinity, melting temperature, crystallization temperature and width at half height of T_m and T_c peaks for iPP and iPP/EPR blends

Sample	Crystallinity (%)		Melting temperature (°C)	Crystallization temperature (°C)	Width at half height of peak (K)	
	X_c	X_c^p			T_m peak	T_c peak
iPP	59	59	164	113	18	9
iPP/EP-88	43	56	171	112	15	9
iPP/EP-81	40	51	170	112	15	9
iPP/EP-74	38	48	170	112	15	8
iPP/EP-66	37	48	170	113	15	8
iPP/EP-16	38 (PP) 2 (PE)	–	174 (PP) 132 (PE)	114	17	9

crystallization peaks overlap, as iPP and PE have nearly the same crystallization temperature (114°C for iPP, 111°C for HDPE).

Wide-angle X-ray diffraction

Wide-angle X-ray scattering (WAXS) patterns for iPP, EP-88 copolymer, iPP/EP-16 and iPP/EP-88 blends are shown in *Figure 11*, where the intensities in arbitrary units are plotted against the diffraction angle 2θ. The diffractograms show that the incorporation of the EP-16 and EP-88 copolymers leads to some changes in the structure of iPP. The intensity of the peak at $2\theta = 16.1°$, which corresponds to the (300) diffraction peak of the β-form (hexagonal phase)[14,15], decreases markedly with the addition of EP-16 and EP-88. The relative amount of the β-form is usually described in terms of the K value, which is defined as:

$$K = \frac{H(300)}{H(300)+H(110)+H(040)+H(130)}$$

where $H(110)$, $H(040)$ and $H(130)$ are the heights of three strong equatorial α-form peaks (110), (040) and (130), and $H(300)$ the height of the strong single β-form peak (300).

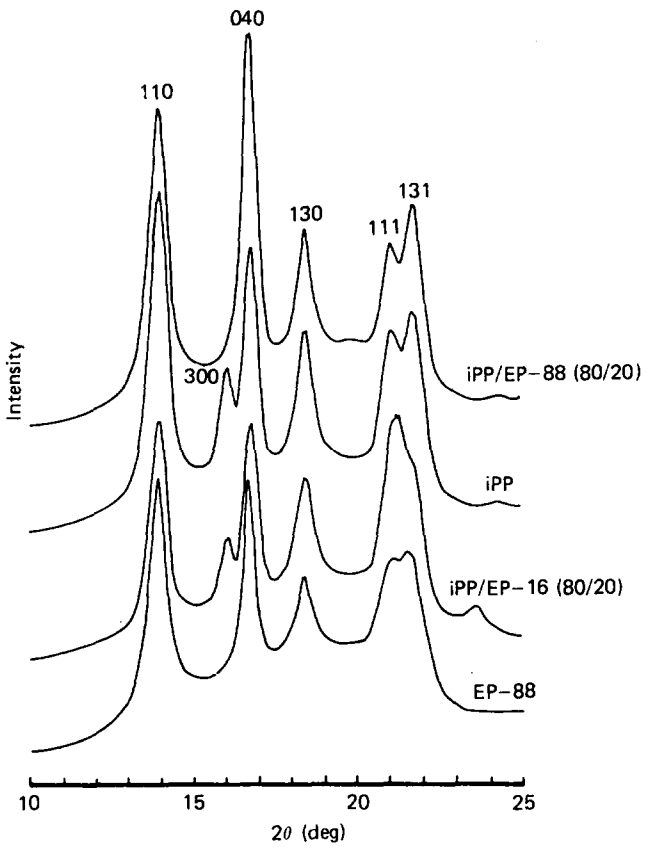

Figure 11 WAXD patterns of iPP, iPP/EP-16, EP-88 and iPP/EP-88

Using this equation we obtained the K values of pure iPP, iPP/EP-16, iPP/EP-88 and EP/88 as follows: 13%, 10%, 0%, 0%, respectively.

It may be concluded that, by incorporation of EP-16 and EP-88 copolymers, the proportion of the monoclinic (α-form) and hexagonal (β-form) phases is modified in the iPP matrix. The proportion of these two forms usually depends on the moulding conditions and the nucleation process[16]. From our experiments the moulding conditions were the same for all specimens. Therefore it can be suggested that EP-16 and EP-88 copolymers show a different effect on the nucleation of α- and β-iPP phases. This different influence is due to the diversity in chemical structure of the two copolymers.

Mechanical tensile properties

The Young's modulus E, tensile yield stress σ_y and the constant stress at cold-drawing σ_c (the stress at the plateau of a stress–strain curve) of iPP/EP-88, 81, 74, 66, 16 copolymer blends are shown in *Table 3*. It may be observed that a decrease of the C_3 content in the copolymer lowers all the parameters in the blends.

This effect can be tentatively explained as follows. First of all, in general 20% of iPP has been substituted by less crystalline copolymers in all the blends. Furthermore from *Table 1* one can observe that on lowering the propylene percentage (C_3) in the copolymers, both the crystallinity content X_c and the glass transition temperature decrease. The diminution of both these parameters renders the system softer and softer, and hence the modulus E, the yield stress σ_y and the stress at cold-drawing σ_c must decrease.

The only exception is the iPP/EP-16 blend where the copolymer has a considerably higher values of X_c but a very low T_g. The effect of increased softness of the amorphous regions can therefore overcome the reinforcing effect of the PE crystallites in the copolymer. Therefore also for this blend E and σ_y decrease further (σ_c is not reported in *Table 1*, since the low compatibility of EP-16 with iPP creates large domains which hamper cold-drawing of the iPP matrix and induce premature rupture before neck formation).

Impact properties

The impact strength R for the iPP/EP-55 and iPP/EP-88 blends is reported as a function of temperature in *Figure 12*. The curves refer to different blend compositions. The iPP homopolymer is taken as the reference material in order to evaluate the impact performance of the blends.

As one can see the impact strength of pure iPP remains almost constant at very low values (over the whole temperature range investigated). Only a very slight enhancement is detected near its glass transition

Table 3 Young's modulus E, tensile yield stress σ_y and the constant stress at cold-drawing σ_c of iPP and iPP/EPR blends

Sample	Composition (iPP/EPR in weight)	C_3 content of EPR (wt%)	$E \times 10^{-3}$ (kg cm^{-2})	$\sigma_y \times 10^{-2}$ (kg cm^{-2})	$\sigma_c \times 10^{-2}$ (kg cm^{-2})
iPP	100/0	–	11.4	3.9	2.8
iPP/EP-88	80/20	92	10.9	3.6	2.7
iPP/EP-81	80/20	86	10.4	3.1	2.4
iPP/EP-74	80/20	81	9.8	2.8	2.2
iPP/EP-66	80/20	74	8.3	2.6	2.2
iPP/EP-16	80/20	22	6.6	2.0	–

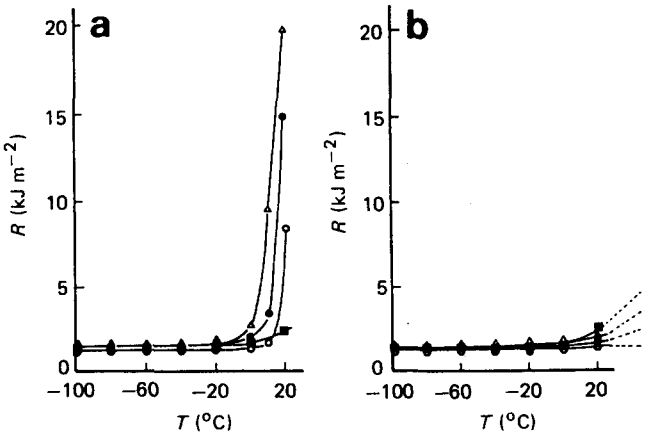

Figure 12 Impact strength R of pure iPP and iPP/EPR blends as a function of testing temperature: (a) iPP/EP-55; (b) iPP/EP-88. Copolymer percentage: ■, 0%; ○, 10%; ●, 15%; △, 20%

temperature. All the corresponding fracture surfaces show the typical appearance of a brittle material.

For the iPP/EP-55 blends (*Figure 12a*) the behaviour at low temperature (up to about 0°C) is similar to pure iPP, but above 0°C a substantial rise in impact strength is achieved. This rise is accompanied by a stress-whitening phenomenon over the entire fracture surface due to a multicraze formation. In contrast, as shown in *Figure 12b* for the iPP/EP-88 blends no enhancement in the R values is observed as the temperature rises. An examination of their fractured surface displays no stress-whitening, indicating that fracture occurs mainly by direct crack formation without crazing, just as in the case of pure iPP. The above findings are in agreement with the morphological observations.

In fact, as shown from the SEM analysis when the C_3 content of the added copolymer is lower, as in the case of EP-55, a dispersed phase of spherical rubbery domains can be observed (see *Figure 2*). These rubbery particles act as sites of stress concentration. Therefore as soon as the stress around the particles overcomes the yield stress of the matrix, a multiple craze mechanism becomes active and an increase in toughening is achieved. The extent of such a phenomenon, as can be expected, increases with enhancing copolymer content.

SEM micrographs demonstrate that in the case of iPP/EP-88 blends this type of toughening mechanism is completely absent insofar as no dispersed phase is present. This finding is due to the high affinity of EP-88 molecules for the iPP matrix. This effect accounts for the lower R values of iPP/EP-88 blends as compared to those observed for the iPP/EP-55 blends.

Properties of fibres

Thermal properties. The parameters X_c, X_c^p, T_m and widths at half height of the T_m peaks of the fibres for the iPP and iPP/EPR blends calculated from the differential scanning thermograms are shown in *Table 4*. As expected the overall d.s.c. crystallinity X_c decreases for the blends with respect to the pure iPP. For fibres of iPP/EPR blends, the X_c values are slightly less than X_c^p. Melting temperatures and widths at half height of melting peaks of fibres of iPP/EPR blends are nearly the same as those of pure iPP fibres.

Such findings could indicate that after stretching the segregation (introduced by the presence of EPR

Table 4 Crystallinity, melting temperature and width at half height of melting peaks of fibres

Sample	Crystallinity (%) X_c	Crystallinity (%) X_c^p	Melting temperature (°C)	Width at half height of melting peak (K)
iPP	65	65	165	15
iPP/EP-88	56	60	163	13
iPP/EP-81	53	55	164	14
iPP/EP-74	49	53	162	13
iPP/EP-66	49	52	164	14

Table 5 Young's modulus E, tensile yield stress σ_y and elongation at break of fibres ε_b of isotropic quenched iPP and iPP/EPR blends

Sample	Composition (iPP/EPR in weight)	C_3 content of EPR (wt%)	$E \times 10^{-3}$ (kg cm^{-2})	$\sigma_y \times 10^{-2}$ (kg cm^{-2})	ε_b (%)
iPP	100/0	–	23.2	14.8	80
iPP/EP-88	80/20	92	21.9	13.9	70
iPP/EP-81	80/20	86	17.6	12.6	50
iPP/EP-74	80/20	81	12.8	10.5	55
iPP/EP-66	80/20	74	10.9	8.6	90

copolymers) between the iPP molecules with steric defects or lower molecular weight and the iPP molecules with higher stereoregularity and higher molecular weight could be recovered to a certain extent. We should remember, in fact, that the fibres are formed through complex morphological rearrangements due to the high mechanical energy input into the very localized regions of the neck. This process transforms the initial spherulitic structure into a new one of fibrillar type.

Mechanical tensile properties. Young's modulus E, tensile yield stress σ_y and elongation at break ε_b of oriented fibres of iPP and iPP/EPR blends are shown in *Table 5*. The values of E and σ_y of iPP/EPR blends decrease with decrease of C_3 content in the copolymers. As for isotropic samples this behaviour can be attributed to the lower crystallinity of the EPR containing C_3 content. In fact during fibre formation the number of tie molecules linking the broken crystallites is fewer the lower the crystallinity constant.

The value of the elongation at break shows a minimum value for the iPP/EP-81 blend. Currently we cannot give any explanation for this last effect.

It was not possible to obtain fibre formation by stretching the iPP/EP-16 blends at room temperature. In fact, specimens broke before the formation of a neck, as previously mentioned. This behaviour further substantiates the strong incompatibility between iPP and EP-16 copolymer (see the section on 'Morphology').

CONCLUSIONS

A thorough investigation of the effect of block EPR copolymers with different C_2/C_3 ratios on the morphology and properties of an isotactic polypropylene has been carried out. The blend properties generally depend on the copolymer composition: in fact an increase of C_3 in the copolymers induces the following structural

changes in the iPP matrix:

(a) a stronger nucleating effect (see optical micrographs);

(b) a higher compatibility (see electron micrographs);

(c) a lower β-content phase;

(d) more perfect crystallites (higher T_m and narrower peaks).

This very remarkable phenomenon is probably due to the ability of all the copolymers to dissolve and extract from the matrix most of the defective iPP chains.

The mechanical tensile properties of both initial unoriented specimens and fibres worsen progressively with respect to iPP the lower the C_3 content.

The opposite holds for the impact properties, which show a slight improvement when the compatibility between iPP and the copolymers decreases (C_3 is lowered).

The behaviour of iPP/EPR blends is very similar to that of HDPE/EPR with respect to the EPR composition. In fact as soon as it comes closer to that of the matrix, the compatibility increases, the mechanical properties improve and the impact resistance diminishes. Also the extractive nature of the copolymers with respect to defective HDPE or iPP molecules is observed in both cases.

The results of the two types of blend, investigated in the present paper and in the previous one[12], are relative to materials obtained at high undercooling. The effect of different crystallization conditions (low undercooling) is presented and discussed in the third paper of this series[13].

ACKNOWLEDGEMENTS

The authors wish to thank Mr L. Serio, Mr V. D. Liello and Mr M. Viola for their help in carrying out the experimental work.

REFERENCES

1 Martuscelli, E., Silvestre, C. and Bianchi, L. *Polymer* 1983, **24**, 1458
2 Martuscelli, E., Silvestre, C. and Abate, G. *Polymer* 1982, **23**, 23
3 Martuscelli, E. *Polym. Eng. Sci.* 1984, **24**, 563; Galeski, A., Pracella, M. and Martuscelli, E. *J. Polym. Sci., Polym. Phys. Edn.* 1984, **22**, 739
4 Bianchi, L., Forte, A., Greco, R., Martuscelli, E., Riva, F. and Silvestre, C. *Kautschuk Gummi* 1984, **34**, 281
5 Bianchi, L., Cimmino, S., Forte, A., Greco, R., Martuscelli, E., Riva, F. and Silvestre, C. *J. Mater. Sci.* 1985, **20**, 895
6 Coppola, F., Greco, R., Martuscelli, E., Kammer, H. W. and Kummerlowe, C. *Polymer* submitted for publication
7 Kumbhoni, K. *J. Polym. Progr. (Plast. Edn.)* 1974, **3**, Aug.–Sept.
8 Spenadel, L. *J. Appl. Polym. Sci.* 1972, **16**, 2375
9 Karger-Kocsis, J., Kallò, A., Szafner, A., Bodor, G. and Sengei, Z. *Polymer* 1979, **20**, 37
10 Danesi, S. and Porter, R. S. *Polymer* 1978, **19**, 448
11 Coppola, F., Greco, R. and Ragosta, G. *Mater. Sci.* 1986, **21**, 1775
12 Greco, R., Mancarella, C., Martuscelli, E., Ragosta, G. and Jinghua, Y. *Polymer* 1987, **28**, 1922
13 Greco, R., Martuscelli, E., Ragosta, G. and Jinghua, Y. *Polymer* submitted for publication
14 Samuels, R. J. and Yec, R. Y. *J. Polym. Sci.* (*A*-2) 1972, **10**, 385
15 Lovinger, A. J., Chua, J. O. and Gryte, C. C. *J. Polym. Sci., Polym. Phys. Edn.* 1977, **15**, 641
16 Norton, D. R. and Keller, A. *Polymer* 1985, **26**, 704